Optics and Laser Technology 106 (2018) 100–106

Contents lists available at ScienceDirect

Optics and Laser Technology

journal homepage: www.elsevier.com/locate/optlastec

Full length article

# Residual aberration correction method of the three-mirror anastigmat (TMA) system with a real exit pupil using freeform surface

Qingyu Meng [a,b,*], Hongyuan Wang [a], Zhiqiang Yan [a]

[a] Research Center for Space Optical Engineering, Harbin Institute of Technology, No. 2 Yikuang Street, Harbin 150080, China
[b] Changchun Institute of Optics, Fine Mechanics and Physics, Chinese Academy of Sciences, No. 3888, Dongnanhu Road, Changchun 130033, China

ARTICLE INFO

*Article history:*
Received 19 March 2017
Received in revised form 23 December 2017
Accepted 31 March 2018
Available online 10 April 2018

*Keywords:*
Geometric optical design
Optical freeform surface
Mirror system design
Aberration compensation

ABSTRACT

The goal of the letter is to reduce the manufacturing and alignment difficulty of a large-scale optical system with a real exit pupil on the premise of ensuring the high-quality imaging. An optical system residual aberration correction method by inserting a quasi-planar freeform mirror (QFM) near the exit pupil position is proposed, and here we define the residual aberration is caused by the reduced tolerance of the manufacturing and alignment. By correction analysis, the mathematical model with the QFM sensitivity matrix as the core has been established. In order to verify the residual aberration correction effectiveness and method of the QFM, a set of real manufactured mirrors shape errors and mirrors positions misalignments are introduced on a well-designed three-mirror-anastigmatic (TMA) system with an aperture of 2 meters, a focal ratio of f/12 and a field of view (FOV) of 1.2° to simulate optical system imaging quality damaged condition, and these errors cause the system imaging degeneration to RMS wavefront error (WFE) 0.331λ. Based on the QFM correction method, the system RMS WFE is corrected from the damaged imaging quality 0.331λ to 0.062λ. The QFM tolerance analysis shows that the QFM has looser precision requirements of manufacturing and alignment. By the verification, it shows this method can correct system residual aberration which caused by mirror manufacturing and alignment errors well at one time, and the TMA system has become less strict in manufacturing and alignment requirements by this way than before. The QFM correction ability and the correction method are effective.



## 1. Introduction

In recent decades, due to the requirements of astrophysics, earth sciences, and planetary physics, the optical system with a large aperture and long focal length which can provide high resolution imaging are widely applied in various space telescopes. The telescope focal length scale is developed from meter-scale to decameter-scale, and more and more telescopes have meters mirrors. However, with the increment of the focal length and the mirror aperture, there is also a relevant increment of the optical system alignment sensitivity and mirror manufacture difficulty substantially, and these problems make us to have to cost more time and budget to achieve an optical system with a larger aperture and longer focal length.

Hubble Space Telescope (HST) is a large space optical telescope with an aperture of 2.4 m and a focal ratio of f/24 which developed by the National Aeronautics and Space Administration (NASA) is a typical example [1]. The optical telescope assembled in the HST is a Ritchey-Chretien system, in order to achieve a high-quality imaging, the ∅2.4 m primary mirror (PM) shape error value is required to achieve RMS 0.014λ at 632.8 nm. The mirror manufacturing processing costs three years to achieve this goal and the mirror manufacturing is extremely costly.

Supernova Acceleration Probe (SNAP) which is a proposed space observatory designed to measure the expansion of the universe and to determine the nature of the mysterious dark energy that is accelerating this expansion. SNAP applies a Korsch type three-mirror-anastigmat (TMA) optical system with an aperture of 2 m and a focal length of 22 m [2]. The primary mirror (PM), secondary mirror (SM) and tertiary mirror (TM) sizes of SNAP are ∅2050 mm, ∅500 mm and ∅730 mm, respectively. On account of the high-quality imaging requirement, the PM, SM and TM manufacturing shape errors distributions are 10 nm, 7.5 nm and 7.5 nm, respectively. Besides, the telescope mirror alignment wavefront errors distributions are 1 nm, 7 nm and 10 nm, respectively. This TMA optical system is faced with extremely strict tolerances of optical elements manufacturing and alignment. In summation, the high-quality imaging requirement brings relevant high-precision

* Corresponding author at: Research Center for Space Optical Engineering, Harbin Institute of Technology, No. 2 Yikuang Street, Harbin 150080, China.
*E-mail address:* mengqy@ciomp.ac.cn (Q. Meng).

https://doi.org/10.1016/j.optlastec.2018.03.035
0030-3992/

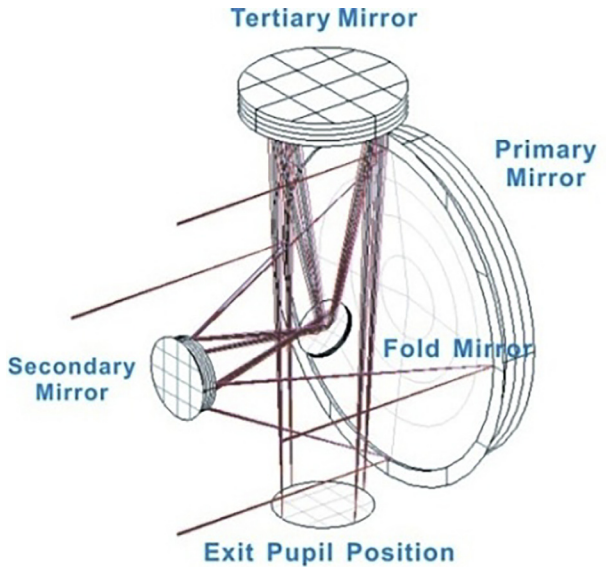


**Fig. 1.** Korsch TMA system.

requirements for a space telescope optical system, and any off-tolerance will lead to the imaging failure. The high-precision mirror milling and polishing is a high-cost and low-efficient work, besides, the high-precision mirror shape error requirement also need the cooperation with a set of high-precision high-cost opto-mechanical structure. Although the computer aided alignment (CAA) [3,4] technique which is an effective method for optical system alignment has been widely used in a mount of telescopes, it cannot lower the alignment precision requirement for the optical system. How to reduce the manufacturing and alignment difficulty of a large-scale optical system on the premise of ensuring the high-quality imaging is this paper desired goal.

In this letter, a residual aberration correction method of an optical telescope with a real exit pupil has been proposed. The goal of the method is aimed at reducing the manufacturing and alignment requirements of a high-precision optical system with a real exit pupil. This method is based on a quasi-planar freeform mirror (QFM) which located at the exit pupil, by solving the QFM freeform coefficients from the QFM sensitivity matrix to compensate the residual aberrations which caused by the mirror manufacturing and misalignment errors. By this method, a residual correction verification of a TMA system with an aperture of 2 m, a focal ratio of f/12 and a field of view (FOV) of ⌀1.2° is given. In this system, in order to achieve a high-quality imaging, the tolerance distributions require the PM, SM and TM shape errors to achieve RMS λ/50, λ/60 and λ/50 at 632.8 nm, respectively, and the TM alignment accuracy is required to achieve a tilt of ±5″ and a decentration of ±10 μm.

For verifying the QFM residual aberration correction effectiveness, simulative errors are added in the system, and the optical system imaging quality is damaged by these errors consequently. By inserting a QFM with the calculated coefficients near the exit pupil position, the system obtains a desired imaging quality which satisfied with the Maréchal criterion. The correction verification result shows that the QFM can correct system residual aberration well at one time. We believe this residual aberration correction method can make the large-scale high-precision optical system has much less strict manufacturing and alignment requirements than before.

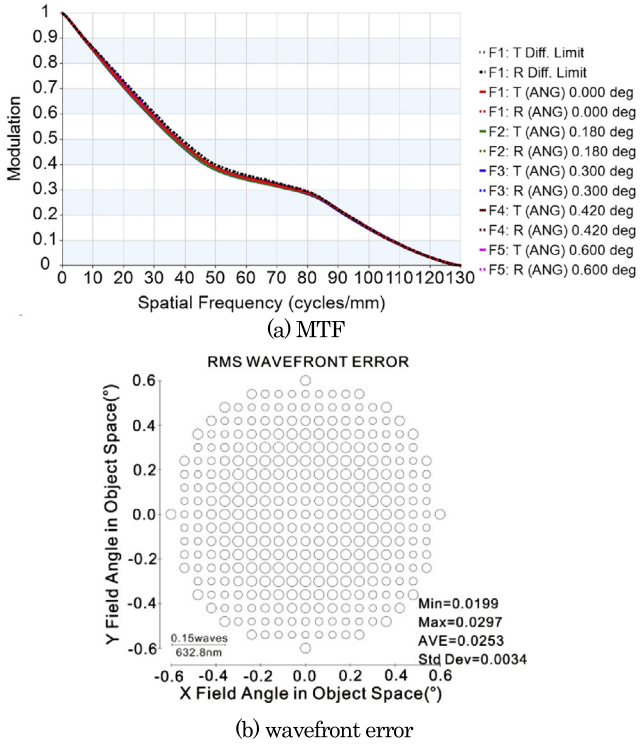


**Fig. 2.** MTF and wavefront error design value.

## 2. Optical system correction analysis and method

### 2.1. Analysis for a typical TMA optical system

The optical systems with a real exit pupil have very important applications, including be convenient for suppressing the stray light, placing a cold stop for infrared system, matching the entrance pupil of the subsequent systems such as subsequent camera or spectrometer systems, and so on [5]. Among the real exit pupil systems, the Korsch type TMA system is a frequently-used significant optical system in telescope [6–8]. In this letter, we design a Korsch type TMA optical system with an aperture of 2 meters, a focal ratio of f/12 and a FOV of 1.2°, the design result is shown in Fig. 1 (the back focal length is drawn briefly), and the configuration parameters are shown in Table 1. The MTF design value is close to the diffraction limit at all spatial frequency which shown in Fig. 2, and the RMS wavefront error (WFE) design value is 0.025λ (λ = 632.8 nm).

According to the Maréchal criterion [9], a well-corrected, diffraction-limited optical system has an RMS WFE not exceeding λ/14, and the majority of the high-resolution optical systems distribute the tolerance based on this criterion. Therefore, the TMA optical system tolerance distribution is shown in Table 2. From the tolerance distribution, we can see the TMA system with a large

**Table 1**
Configuration parameters.

| | Surface type | Radius (mm) | Distance (mm) | Conic | Mirror size (mm) |
|---|---|---|---|---|---|
| PM | Conic | −3955.397 | −1577.66 | −0.9759 | ⌀2000 |
| SM | Conic | −1600.235 | 950 | −8.3449 | ⌀450 |
| FM | Plane | – | −1457.19 | 0 | ellipse 200 × 300 |
| TM | Conic | 2759.53 | 9751.56 | −0.6055 | ⌀1000 |

**Table 2**
Tolerance distribution.

| Mirror | Manufacturing | | | Alignment | | | |
|---|---|---|---|---|---|---|---|
| | Shape error (λ) | ΔR (mm) | ΔK | Tilt (″) | | Decentration (μm) | |
| | | | | X | Y | X | Y |
| PM | 1/50 | ±2 | ±0.0003 | Reference | Reference | Reference | Reference |
| SM | 1/60 | ±1 | ±0.0005 | Compensator | Compensator | Compensator | Compensator |
| FM | 1/80 | Null | Null | ±5 | ±5 | Null | Null |
| TM | 1/50 | ±1.5 | ±0.0005 | ±5 | ±5 | ±10 | ±10 |

**Table 3**
Alignment sensitivity analysis.

| Misalignment | 1″ | 2″ | 1 μm | 2 μm |
|---|---|---|---|---|
| *SM* | | | | |
| RMS WFE (λ) | 0.0295 | 0.0404 | 0.0257 | 0.0268 |
| Increment (λ) | 0.0043 | 0.0152 | 0.0005 | 0.0016 |
| Ratio (%) | 17.06 | 60.32 | 1.98 | 6.35 |
| TM | | | | |
| RMS WFE (λ) | 0.0259 | 0.0279 | 0.0253 | 0.0253 |
| Increment (λ) | 0.0007 | 0.0027 | 0.0001 | 0.0001 |
| Ratio (%) | 2.78 | 10.71 | 0.4 | 0.4 |

**Table 4**
Optical system misalignment simulation data.

| Mirror | RMS shape error (λ) | Tilt (″) | | Decentration (μm) | |
|---|---|---|---|---|---|
| | | X | Y | X | Y |
| PM | 0.046 | Reference | | Reference | |
| SM | 0.025 | 5 | −5 | −5 | 5 |
| TM | 0.030 | −20 | 20 | 40 | −40 |

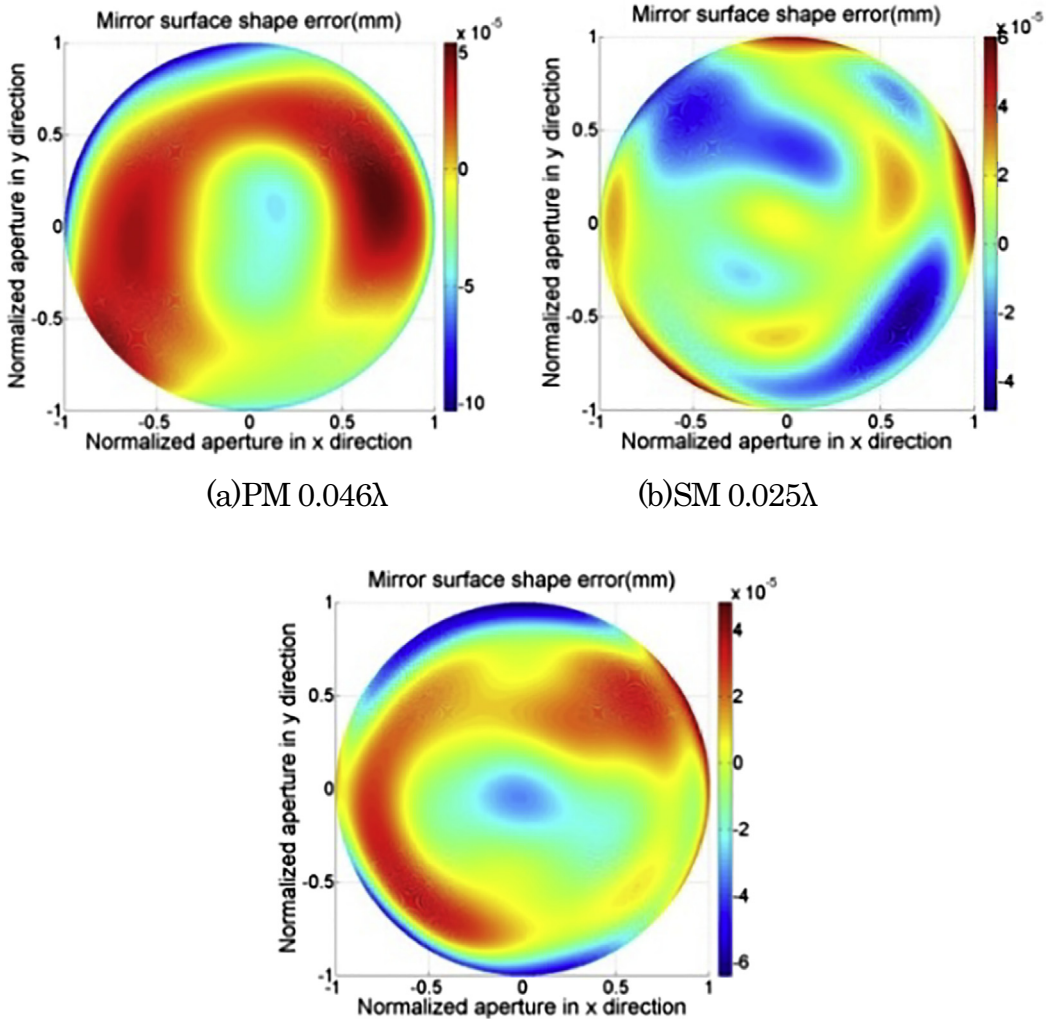


**Fig. 3.** Mirror surface simulated shape error, measured data by Zygo (RMS value, λ = 632.8 nm).

aperture and a long focal length has strict requirements in mirror manufacturing and alignment. The ∅2 m PM, ∅0.45 m SM and ∅1 m TM surface shape errors are requested to achieve RMS λ/50, λ/60 and λ/50, respectively. Such high-precision mirror shape error requirements of so large aperture mirrors will need a high cost and a long time to accomplish, and the such mirrors also need a precise cooperation with a set of high-precision high-cost opto-mechanical structure. Furthermore, the system also requires a high-precision alignment to be achieved which shown in Table 2, for a meter-scale TM, it is a strict alignment technical index with a tilt of ±5″ and a decentration of ±10 μm. During the alignment process, although the SM position can be set as a compensator, it has a high sensitivity which shown in Table 3. Based on above analysis, on the premise of ensuring the optical system high-quality imaging, to lower the manufacturing and alignment difficulty is our target.

### 2.2. Correct analysis

On the basis of nodal aberration theory (NAT) [10], when there is a surface at the pupil, the beam footprint is the same for all the field points, so all fields receive the same wavefront contributions from the pupil surface. When there is a certain distance between the surface and the pupil, then all fields receive the different wavefront contributions from the pupil surface. It has been illustrated that a phase mask can be introduced at the pupil in order to reduce the effect of aberrations.

In the optical system design process, one type negative aberration can balance out the same type positive aberration, and this performance illustrates that one type of surface can balance out the same kind of aberration generated in the overwhelming majority of cases [11]. Based on these principles, a wavefront correction element or a phase mask can be inserted near the exit pupil where usually as the smallest diameter position in the optical path, by the modulation of the wavefront compensations generated by this wavefront correction element to correct the system wavefront distortion caused by the mirror manufacturing and system misalignment errors. Under the guidance of this philosophy, the system residual aberration can be well corrected at one time, and the mirror manufacturing and alignment technical requirements can be lowered. By just introducing one wavefront correction element to reduce multiple mirrors technical requirements is a high cost-effective work.

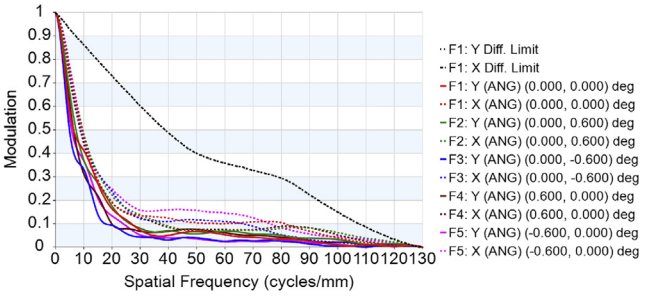


(a) MTF

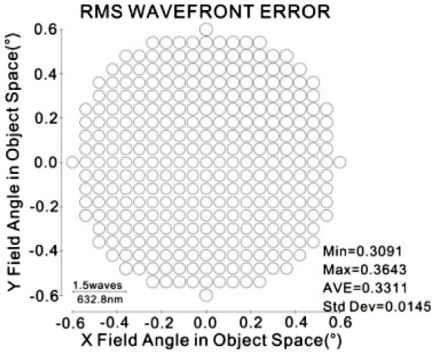


(b) wavefront error

**Fig. 4.** MTF and wavefront error performance caused by mirror shape and misalignment errors.

Freeform surfaces have strong aberration correction ability which benefitted from its abundant design freedom [12]. Freeform surfaces have been successfully applied in several imaging systems and illumination systems [13–16]. With the progress of optical manufacturing, more high-order freeform surfaces which are adept in high-order aberration correction can be milled. A large number of design results show that the freeform surfaces can assist the optical system which with high technological indicators to achieve a high-quality imaging closed to the diffraction limit [17–19].

Based on above analysis, if we place a quasi-planar freeform mirror (QFM) near the exit pupil position as the wavefront correct element, the optical system residual aberration generated by the mirror manufacturing and misalignment errors can be corrected well by modulating the QFM freeform coefficients. The goal of reducing the manufacturing and alignment difficulty of a large-scale optical system on the premise of ensuring the high-quality imaging will be achieved.

### 2.3. Mathematical model

For the mirror manufacturing error, the shape error can be measured by interferometer, and the data can be expressed by Zernike coefficients. We can use optical design software to re-optimize the optical system by designing the QFM freeform coefficients to compensate system WFE caused by mirror shape error [20]. Besides, misalignment error has an greatly influence on the system imaging quality, but the misalignment data as an unknown quantity cannot be obtained exactly, so we cannot obtain the freeform coefficients by re-optimization method to compensate system WFE caused by misalignment. We should adopt other method to calculate an equivalent WFE compensation generated by the QFM to compensate WFE caused by a set of unknown misalignments.

By analyzing, a small increment of a certain freeform coefficient of the QFM will generate a small WFE, and it will cause a small increment of several wavefront Zernike coefficients. Within a certain range, there is a linear relationship between each freeform coefficient variation and each wavefront Zernike aberration variation of each field. The relationship can be expressed in matrix as following:

$$S\Delta M = -\Delta F(r) \tag{1}$$

$S$ is the QFM sensitivity matrix,
$\Delta M$ is the QFM freeform coefficients,
$\Delta F(r)$ is the wavefront aberrations difference between the actual optical system (damaged by the manufacturing and misalignment errors) and the well-designed one.

The sensitivity matrix is shown in Eq. (2), and here the QFM surface type is defined as Fringe Zernike polynomials.

$$S = \begin{pmatrix} \frac{\partial F(1)_{Z1}}{\partial M_{Z1}} & \frac{\partial F(1)_{Z1}}{\partial M_{Z2}} & \cdots & \frac{\partial F(1)_{Z1}}{\partial M_{Zn}} \\ \vdots & \vdots & \ddots & \vdots \\ \frac{\partial F(1)_{Zm}}{\partial M_{Z1}} & \frac{\partial F(1)_{Zm}}{\partial M_{Z2}} & \cdots & \frac{\partial F(1)_{Zm}}{\partial M_{Zn}} \\ \frac{\partial F(2)_{Z1}}{\partial M_{Z1}} & \frac{\partial F(2)_{Zm}}{\partial M_{Z2}} & \cdots & \frac{\partial F(2)_{Zm}}{\partial M_{Zn}} \\ \vdots & \vdots & \ddots & \vdots \\ \frac{\partial F(r)_{Zm}}{\partial M_{Z1}} & \frac{\partial F(r)_{Zm}}{\partial M_{Z2}} & \cdots & \frac{\partial F(r)_{Zm}}{\partial M_{Zn}} \end{pmatrix} \tag{2}$$

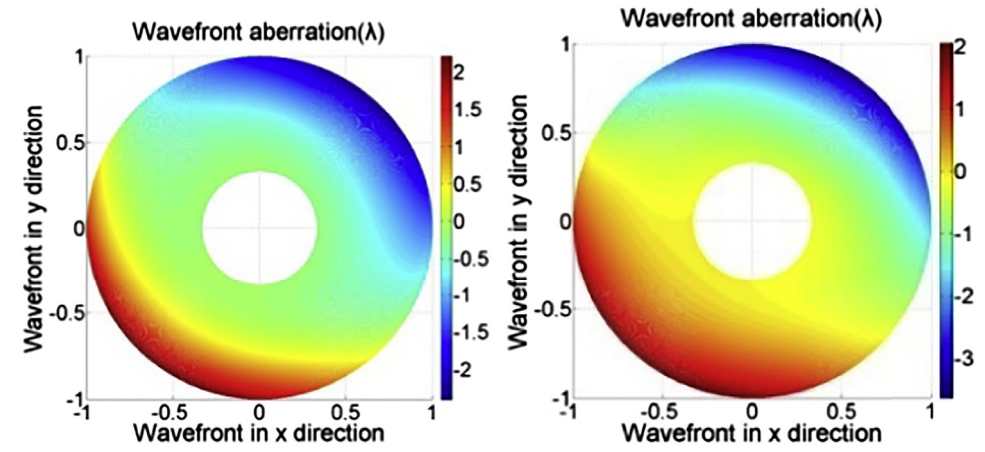


(a) (0°, 0°) (b) (0°, 0.6°)

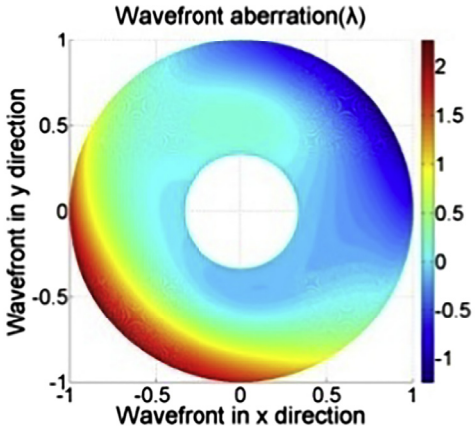


(c) (0°, -0.6°)

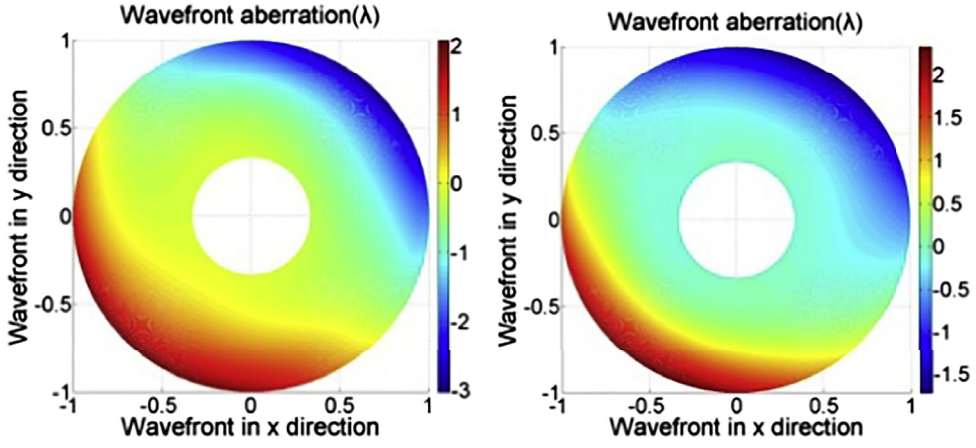


(d)(0.6°,0°) (e)(-0.6°,0°)

**Fig. 5.** Wavefront aberration pseudo-color images.

$M_{Zn}$ is each QFM freeform coefficient, and n is the QFM freeform coefficient sequence number,
$F(r)_{Zm}$ is each wavefront Fringe Zernike aberration coefficient of each filed, $r$ is field sequence number and $m$ is the Fringe Zernike coefficient sequence number,
$\partial F(r)_{Zm}/\partial M_{Zn}$ is the partial differential of $M_{Zn}$ to $F(r)_{Zm}$, and it can be replaced by $\delta F(r)_{Zm}/\delta M_{Zn}$ in linear interval.

$\Delta M$ is shown in Eq. (3), and $\Delta M_{Zn}$ is the each QFM freeform coefficient which is the solution we want to obtain.

$$\Delta M = \begin{pmatrix} \Delta M_{Z1} \\ \vdots \\ \Delta M_{Zn} \end{pmatrix} \tag{3}$$

$\Delta F(r)$ is shown in Eq. (4) as following:

$$\Delta F(r) = \begin{pmatrix} \Delta F(1)_{Z1} \\ \vdots \\ \Delta F(1)_{Zm} \\ \Delta F(2)_{Zm} \\ \vdots \\ \Delta F(r)_{Zm} \end{pmatrix} = \begin{pmatrix} F(1)_{Z1} \\ \vdots \\ F(1)_{Zm} \\ F(2)_{Zm} \\ \vdots \\ F(r)_{Zm} \end{pmatrix} - \begin{pmatrix} F(1)_{Z01} \\ \vdots \\ F(1)_{Z0m} \\ F(2)_{Z0m} \\ \vdots \\ F(r)_{Z0m} \end{pmatrix} \quad (4)$$

$\Delta F(r)_{Zm}$ is the increment of wavefront aberrations Zernike coefficient of each field,
$F(r)_{Z0m}$ is the wavefront aberrations Zernike coefficient design value of each field.

We use the 2nd to 36th QFM Fringe Zernike polynomial coefficients to correct system residual aberrations, so n number is set as 35. And we sample 1st to 36th wavefront Fringe Zernike aberration coefficients to establish the equation, so m number is set as 36. When m > n, Eq. (1) is an over-determined equation, the solution can be solved by the simple least-squares (LS) method, and the solution can be expressed as following:

$$\Delta M = (S^T S)^{-1} S^T \Delta F(r) \quad (5)$$

## 3. Correction verification

### 3.1. Correction example

To verify the residual aberration correction effectiveness of the QFM and the correction method, we use the designed Korsch type TMA system to accomplish the correction simulation. Three sets of real manufactured mirror shape errors (shown in Fig. 3) are adopted to simulate the PM, SM and TM shape errors, and the data are measured by Zygo interferometer. The real mirror shape errors are not satisfied with the system tolerance distribution shown in Table 2. The three sets of shape errors are caused by numerous factors including mirror manufacturing, opto-mechanical structure stress-deformation, and so on. Furthermore, a large random misalignment of the SM and TM are introduced in the system to simulate the system position mis-adjustments situation. The data are shown in Table 4.

Consequently, the system imaging quality is damaged by these errors, the system RMS WFE has dipped to 0.331λ and the MTF is shown in Fig. 4.

In this TMA system, the PM is set as the entrance pupil, and its shape error will generate the same aberration contribution for every filed. However, the shape errors and positions mis-adjustments of the SM, TM will generate the different contributions for every field, thus the QFM should not be located just at the exit pupil position exactly, and it should had better to have a small certain distance from the exit pupil. Here, the QFM position is set 2600 mm behind the TM, and the QFM position has been planed already during the system design process. The QFM aperture is ∅600 mm which is close to exit pupil size.

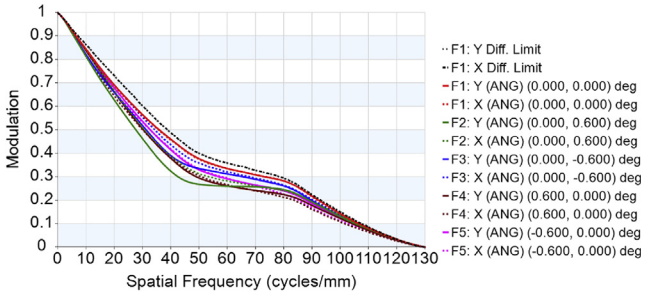


(a) MTF

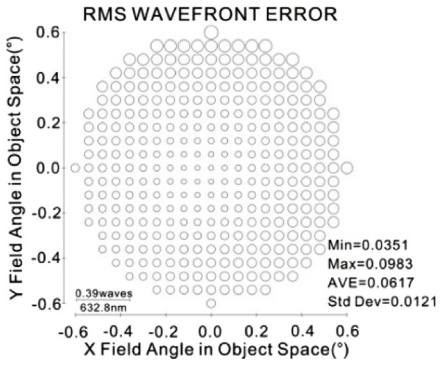


(b) wavefront error

**Fig. 6.** MTF and wavefront error performance with QFM correction.

For obtaining Eq. (5) solution, the wavefront Fringe Zernike aberration coefficients of each field should be sampled firstly. The (0°, 0°), (0°, 0.6°), (0°, −0.6°), (0.6°, 0°) and (−0.6°, 0°) are set as the sampling fields. The wavefront aberration pseudo-color images of each field are shown in Fig. 5. Although the TMA system is coaxial, the wavefront is asymmetrical about the circular FOVs because of the misalignment. It can prove that the application of freeform surface which can correct asymmetrical aberration is suitable.

Based on above samplings, the ΔF(r) is obtained. Then the QFM freeform coefficients ΔM is solved and the coefficients are shown in Table 5. Benefited from the correction of the QFM, the system RMS WFE achieves 0.062λ which is satisfied with the Maréchal criterion, and the MTF and wavefront performance are shown in Fig. 6. The result shows that the QFM correction ability and the correction method are effective.

### 3.2. QFM tolerance analysis

Based on the system WFE correction result 0.062λ, the QFM tolerance has been analyzed. The QFM tolerance analysis shows

**Table 5**
QFM FRINGE Zernike coefficient.

| | | | | | |
|---|---|---|---|---|---|
| Z1 | Z2 | Z3 | Z4 | Z5 | Z6 |
| 0.000e+00 | −1.339e−1 | −2.523e−1 | 8.675e−6 | −1.753e−5 | 6.327e−6 |
| Z7 | Z8 | Z9 | Z10 | Z11 | Z12 |
| −1.424e−4 | −2.243e−4 | 3.127e−5 | 3.660e−6 | −2.944e−6 | 2.512e−5 |
| Z13 | Z14 | Z15 | Z16 | Z17 | Z18 |
| −6.833e−6 | −6.874e−6 | −1.689e−6 | −4.851e−6 | 1.925e−5 | 1.967e−6 |
| Z19 | Z20 | Z21 | Z22 | Z23 | Z24 |
| −5.136e−6 | −2.123e−6 | 1.048e−5 | −9.479e−6 | −1.877e−6 | 1.242e−5 |
| Z25 | Z26 | Z27 | Z28 | Z29 | Z30 |
| 9.987e−06 | 3.399e−6 | −9.388e−6 | 5.255e−6 | −1.223e−6 | −1.078e−6 |
| Z31 | Z32 | Z33 | Z34 | Z35 | Z36 |
| −7.696e−6 | 7.655e−7 | 2.804e−6 | −5.600e−8 | −7.450e−7 | 8.310e−7 |

**Table 6**
QFM tolerance analysis.

| Shape error (λ) | Tilt (′) | | Decent (mm) | | Rotation (°) |
|---|---|---|---|---|---|
| | X | Y | X | Y | |
| 1/35 | ±3 | ±3 | ±0.5 | ±0.5 | ±1 |

that the QFM has looser precision requirements of manufacturing and alignment.

Because the QFM has little focal power, so it is insensitive. During the QFM alignment process, the image plane is set as the compensator, and its position and inclination angle can be adjusted for system alignment. Based on the λ/14 Maréchal criterion, the QFM tolerance is shown in Table 6. The QFM shape error requirement is λ/35, and the technical index is not hard to achieve for a plane mirror. The QFM position tolerance are tilt ±3′, decentration ±0.5 mm and rotation ±1°, respectively, which are easy to achieve relatively. Because the QFM assumes responsibility for aberration correction assignment, it results in an optical form that not only higher performance but also simultaneously less sensitive to alignment, the sensitivity of other mirrors is also decreased. Taking the SM tilt sensitivity for an example, it has been reduced by more than 10%.

## 4. Conclusion

In this letter, an optical system residual aberration correction method based on the quasi-planar freeform mirror is proposed. The goal is to reduce the manufacturing and alignment difficulty of a large-scale optical system with a real exit pupil on the premise of ensuring the high-quality imaging. In the verification correction process, the sensitivity matrix of a well-designed TMA system based on the relationship between freeform coefficient variation and wavefront Zernike aberration variation of each field is established. The manufacturing and alignment errors are introduced in the TMA system, and it causes the system imaging degeneration to RMS WFE 0.331λ. By wavefront aberration sampling, the QFM freeform coefficients are solved using DLS method. Benefited from the correction of the QFM, the system RMS WFE achieves 0.062λ which is satisfied with the Maréchal criterion.

The verification shows that this method can correct system residual aberration which caused by mirror manufacturing and alignment errors well at one time, it can make the TMA system has much less strict manufacturing and alignment requirements than before, and the QFM correction ability and the correct method are effective. The analysis shows that the QFM has a looser requirement of manufacturing and alignment, and to some extent the QFM reduces the system sensitivity. The method of using a QFM to reduce the difficulties in manufacturing and alignment of the large-scale optical system is effective.

## Acknowledgments

This work was supported by the National Natural Science Foundation of China (NSFC) (Grant No. 61705220).

## References

[1] NASA, The Hubble Space Telescope Optical System Failure Report, 1990.
[2] M. Sholl, M. Lampton, G. Aldering, et al., Snap telescope, in: Proc. SPIE 5487 1473-1483, 2004.
[3] J.W. Figoski, Alignment and test results of the QuickBird telescope using the ball optical system test facility, in: Proc. SPIE 3785 99-108, 1999.
[4] H. Yang, S. Kim, Y. Lee, J. Song, H. Rhee, H. Lee, J. Lee, I. Lee, S. Kim, Computer aided alignment using Zernike coefficients, Proc. SPIE 6293 (2006) 62930I.
[5] T. Yang, J. Zhu, G. Jin, Starting configuration design method of freeform imaging and afocal systems with a real exit pupil, Appl. Opt. 55 (2016) 345–353.
[6] D. Korsch, Anastigmatic three-mirror telescope, Appl. Opt. 16 (1977) 2074–2077.
[7] D. Korsch, Closed form solution for three-mirror telescopes, corrected for spherical aberration, coma, astigmatism, and field curvature, Appl. Opt. 11 (1972) 2986–2987.
[8] L.G. Cook, The last three-mirror-anastigmat (TMA)?, Critical Reviews of Optical Science and Technology, SPIE, CR41, 1992, pp. 310–324.
[9] M. Bueeler, M. Mrochen, T. Seiler, Maximum permissible lateral decentration in aberration-sensing and wavefront-guided corneal ablation, J. Cataract Refract. Surg. 29 (2003) 257–263.
[10] K. Fuerschbach, J.P. Rolland, K.P. Thompson, Extending Nodal aberration theory to include mount-induced aberrations with application to freeform surfaces, Opt. Express 20 (2012) 20139–20155.
[11] Q. Meng, H. Wang, K. Wang, Y. Wang, Z. Ji, D. Wang, Off-axis three-mirror freeform telescope with a large linear field of view based on an integration mirror, Appl. Opt. 55 (2016) 8962–8970.
[12] K.P. Thompson, J.P. Rolland, Freeform optical surface a revolution in imaging optical design, Opt. Photon. News 23 (6) (2012) 30–35.
[13] H. Wang, X. Li, P. Ge, Design of an optical lens combined with a total internal reflection (TIR) freeform surface for a LED front fog lamp, Opt. Laser Technol. 88 (2017) 11–16.
[14] H. Wu, X. Zhang, P. Ge, Double freeform surfaces lens design for LED uniform illumination with high distance-height ratio, Opt. Laser Technol. 73 (2015) 166–172.
[15] H. Wu, X. Zhang, P. Ge, Design method of a light emitting diode for lamp based on a freeform reflector, Opt. Laser Technol. 72 (2015) 125–133.
[16] T. Yang, J. Zhu, G. Jin, Design of a freeform, dual fields-of-view, dual focal lengths, off-axis three-mirror imaging system with a point-by-point construction-iteration process, Chin. Opt. Lett. 14 (2016) 100801.
[17] Q. Meng, W. Wang, H. Ma, J. Dong, Easy-aligned off-axis three-mirror system with wide field of view using freeform surface based on integration of primary and tertiary mirror, Appl. Opt. 53 (2014) 3028–3034.
[18] T. Yang, J. Zhu, W. Hou, G. Jin, Design method of freeform off-axis reflective imaging systems with a direct construction process, Opt. Express 22 (2014) 9193–9205.
[19] W. Hou, J. Zhu, T. Yang, G. Jin, Construction method through forward and reverse ray tracing for a design of ultra-wide linear field-of-view off-axis freeform imaging systems, J. Opt. 17 (2015) 055603.
[20] H.J. Jeong, G.N. Lawrence, Auto-alignment of a three-mirror, off-axis telescope: reverse optimization, Proc. SPIE 996 (1988).